Published in final edited form as:
Mol Pharm. 2013 October 7; 10(10): . doi:10.1021/mp4003046.

Absolute Quantification of Aldehyde Oxidase Protein in Human Liver Using Liquid Chromatography-Tandem Mass Spectrometry

John T. Barr[†], **Jeffrey P. Jones**[†,*], **Carolyn A. Joswig-Jones**[†], and **Dan A. Rock**[‡]

[†]Department of Chemistry, Washington State University, P.O. Box 644630, Pullman, Washington 99164-4630

[‡]Department of Pharmacokinetics and Drug Metabolism, Amgen Inc., 1201 Amgen Court West, Seattle, Washington 98119

Abstract

The function of the enzyme human aldehyde oxidase (AOX1) is uncertain, however, recent studies have implicated significant biochemical involvement in humans. AOX1 has also rapidly become an important drug metabolizing enzyme. Until now, quantitation of AOX1 in complex matrices such as tissue has not been achieved. Herein, we developed and employed a trypsin digest and subsequent liquid chromatography tandem mass spectrometry analysis to determine absolute amounts of AOX1 in human liver. E. coli expressed human purified AOX1 was used to validate the linearity, sensitivity, and selectivity of the method. Overall, the method is highly efficient and sensitive for determination of AOX1 in cytosolic liver fractions. Using this method, we observed substantial batch-to-batch variation in AOX1 content (21-40 pmol AOX1/mg total protein) between various pooled human liver cytosol preparations. We also observed inter batch variation in V_{max} (3.3-4.9 nmol min^{-1} mg^{-1}) and a modest correlation between enzyme concentration and activity. In addition, we measured a large difference in k_{cat}/K_m, between purified (k_{cat}/K_m of 1.4) and human liver cytosol (k_{cat}/K_m of 15-20) indicating cytosol to be 11-14 times more efficient in the turnover of DACA than the E. coli expressed purified enzyme. Finally, we discussed the future impact of this method for the development of drug metabolism models and understanding the biochemical role of this enzyme.

Keywords

Aldehyde Oxidase; AO; AOX1; protein quantification; drug metabolism; kinetics; mass spectrometry

Humans express a single aldehyde oxidase enzyme known as AOX1 (EC1.2.3.1), that, like xanthine oxidase, is a member of the molybdo-flavoenzyme family. [1] The AO holoenzyme is a cytosolic homodimer, and each 150 kDa monomer is characterized by three separate domains: the 20 kDa N-terminal domain that has two distinct [2Fe-2S] clusters, the 40 kDa central domain that has FAD and the 80 kDa C-terminal domain which binds molybdenum cofactor (MoCo) with an equatorial sulfur-ligand that is essential for enzyme activity.

Although the exact physiological function of AOX1 in human remains unclear, a number of studies have reported findings that implicate significant biological importance for this enzyme in humans. There is evidence for the involvement of AOX on lipid disposition [2-4] as well metabolism of other endogenous substrates such as retinaldehyde [5] and pyridoxal. [6]

[*]Correspondence to: Jeffrey Jones, Department of Chemistry, Washington State University, P.O. Box 644630, Pullman, Washington 99164-4630, Phone 509-592-8790, jpj@wsu.edu.

While the native substrate remains uncertain, the terminal electron acceptor is oxygen, leading to the production of reactive oxygen species (ROS) such as superoxide radical anion or hydrogen peroxide. ROS generated by AOX1 may be important in cellular redox stresses, toxicities, and various human disease states. [7] One such hypothesized toxicity is the correlation of AOX1 activity with the neurodegenerative disease amyotrophic lateral sclerosis. [8] Generation of excess ROS by AOX1 may also contribute to alcohol-induced liver injury. [9] Finally, a recent study has also determined that AOX1 contributes to hepatic injury by chloroform, carbon tetrachloride, and thioacetamide, compounds known to generate ROS. [10]

While historically AOX1 has played a minor role in drug metabolism, recently a number of drugs have failed in clinical trials as a result of AOX1 metabolism. [11-13] The major reason for the failures is poor allometric scaling from preclinical species to humans. [14] This is exacerbated by the use of human microsomal fractions for *in vitro* screening, since AOX1 is a cytosolic enzyme. Furthermore, when human cytosol is used it seems to give variable results from different preparations. The origins of the variations are not known, but the phenotypic variation from common SNPs is not large, [15] and this should be overcome by the use of pooled cytosolic preparations. Hepatocytes also appear to be an alternative to human liver cytosol, [16] but are cost-prohibitive for high throughput screening and appear to have variable activity. Finally, expression and purification of AOX1 has been accomplished, but the overall yield is modest [15, 17] and cofactor incorporation is incomplete. [15] Thus at this time human cytosol is the most attractive source of enzyme. However, since the amount of AOX1 in human cytosol is not known, a rapid method for protein quantification would be valuable for standardization of each AOX1 lot.

To aid in AOX1-related studies in drug metabolism, biochemistry and disease states we have developed a rapid mass spectrometry (MS) method for the quantification of human aldehyde oxidase. Unique peptide fragments from the trypsin digest of AOX1 are identified and a synthetic peptide standard is used to determine the amount of AOX1 in human cytosol from different human liver samples. Herein, we also apply this approach to investigate batch-to-batch variation between commercial HLC as well as the efficiency differences between recombinant purified enzyme with that from a native source.

Experimental Procedures

Materials

Human liver cytosol (pooled from individual donors of mixed gender) was purchased from BD Biosciences (Franklin Lakes, NJ). Guinea pig liver cytosol was purchased from Xenotech LLC (Lenexa, KS). Sequence grade trypsin was acquired from Promega (Madison, WI). The synthetic peptide standard (H-Met-Tyr-Lys-Glu-Ile*-Asp-Gln-Thr-Pro-Tyr-Lys-Gln-Glu-NH_2) with heavy isotope labeling (Ile*= U-$^{13}C_6$) was obtained from Anaspec (Fremont, CA). 2-methyl-4(3H)-quinazolinone (internal standard used in kinetics assays) was purchased from Sigma-Aldrich (St. Louis, MO). N-[(2-dimethylamino)ethyl]acridine-4-carboxamide (DACA) was synthesized according to previously published methods. [18] DACA-9(10H)-acridone was kindly provided by Dr. William A. Denny from University of Auckland (Auckland, New Zealand). All other reagents used were analytical grade or better.

Cytosol Digestion Procedure

In order to determine the human AOX1 levels, an efficient, simple digestion method was developed. Human liver cytosol (25 μL of 20 mg/mL stock) was mixed with a denaturing solution containing 8 M urea and 2mM DTT (25 μL, 4 M urea, 1mM DTT final

concentration) and incubated at 60 °C for 60 minutes. The mixture was subsequently diluted with 25 mM sodium bicarbonate buffer containing 100 nM peptide internal standard (pH 8.4, final 250 μL). Sequence grade trypsin (20 μL of a 0.5 μg/μL solution) was added (1:50 protein to protein ratio of trypsin to cytosol) and incubated overnight at 37 °C. Aliquots of the digested peptide solution were terminated by adding an appropriate amount of 50% v/v trifluoroacetic acid (TFA) in water such that the final concentration was 10% TFA v/v. Samples were subsequently vortexed and centrifuged (1460 g for 10 minutes) prior to LC-MS/MS analysis.

Determination and Selection of AOX1 Peptide Candidates

Samples were immediately analyzed by LC MS/MS. An Accela 1250 HPLC system coupled to an HTS PAL autosampler (LEAP Technologies, Carrboro, NC) interfaced with an LTQ-Orbitrap Velos mass spectrometer (Thermo Fisher Scientific, Bremen, Germany) was used for tryptic peptide analysis. Peptide samples were injected onto a Phenomenex Jupiter C18 column (3 Qm, 2.1 × 150 mm; Torrance, CA) using a flow rate of 0.2 mL/min, with a portion of the column elute (20%) diverted to the mass spectrometer. Mobile phase consisted of 0.05% formic acid in water (A) and 0.05% formic acid in acetonitrile (B). Initial conditions were 98% A, with a linear gradient: 2% B for 2 min, 2–95% B over 35 min, and 95% B for 5 min. Ions were detected in positive mode; peptide masses and fragments were acquired in SRM onn the FT-Orbitrap. Fragment ion spectra acquired from collision-induced dissociation (CID) were produced using 35% collision energy and a 1.0 Da isolation window. Peptides of interest were extracted and analyzed with Quant Browser (Thermo Scientific, San Jose, CA).

HPLC-ESI-MS/MS Quantitation Assay

Digested samples were analyzed using an 1100 series high performance liquid chromatography system (Agilent Technologies, Santa Clara, CA) coupled to an API 4000 tandem mass spectrometry system manufactured by Applied Biosystems/MDS Sciex (Foster City, CA) with a turbospray ESI source operating in positive ion mode. A sample volume of 5 μL was injected onto the column, and chromatography was performed on a HALO C18 column (2.1 × 150 mm, 2.7 μm; Advanced Materials Technology, Wilmington, DE).

Mobile phases comprised 0.05% formic acid and 0.2% acetic acid in water (A), and 90% acetonitrile, 9.9% water, and 0.1% formic acid (B). Using a flow rate of 200 μL/min, the column was equilibrated at initial conditions of 98% mobile phase A for 2 min. Chromatographic separation was performed using a linear gradient over the next 35 min to 5% mobile phase A, and was held at 5% A for 5 minutes. Mobile phase A was then immediately ramped back to 98 % and held constant for an equilibration time of 5 min. The total chromatographic assay time was 47 min per sample, and the retention times for internal standard (IS) and analyte peaks were 10.2 min.

Three MRM transitions were selected for both the IS and native peptide. Compound parameters were optimized as follows: declustering potential, 70; entrance potential, 10; collision energy, 30; collision cell exit potential, 15. Source parameters used were as follows: collision gas, 4; curtain gas, 15; ion source gas 1, 50; ion source gas 2, 5; ion source voltage, 4000; source temperature, 400. Since the native and IS peptides behave identically in MS conditions (ie. in terms of signal response and fragmentation), the native peptide was quantitated by simply comparing the native peak area to the IS peak area of known concentration.

Preparation of Purified AOX1

AOX1 was prepared according to the methods described previously. [17] Briefly, human AOX1 was overexpressed as a N-terminal hexa-His tagged in TP-1000 [19] E. coli cells (a gift from John Enemark's laboratory, University of Arizona). Cells were lysed and partially purified using a 1-ml HiTrap Chelating HP column (GE Healthcare, Little Chalfont, Buckinghamshire, UK). Upon purification, the protein was dialyzed into 100 mM potassium phosphate buffer, pH 7.4 and stored at 80 °C prior to use.

Quantitation of Purified AO by UV assay

UV spectra of air oxidized purified AO samples were taken using an Agilent 8453 UV-Vis spectrometer (Agilent Technologies, Santa Clara, CA). The AO concentration was calculated using the absorbance at 450 nm and the extinction coefficient of 34.7 cm^{-1} mM^{-1}. [20]

Determination of Method Detection Limit (MDL) for MS Quantitation

For calculating MDL, a repeat injection approach was used as described previously. [21] In short, a diluted sample of purified AO was digested and the peak area was measured multiple times. MDL was calculated using the following formula:

$$\mathrm{MDL} = S_{\bar{x}} \quad \mathrm{T}_{\alpha}$$

Where S_x is equal to the standard deviation of the mean for peak area and T_α is the value chosen from a t-table for n=5 at a 99% confidence interval.

Enzyme Kinetics

Saturation kinetics assays were performed using DACA as a probe substrate. All incubations were performed in 25 mM potassium phosphate buffer (pH 7.4) with 7 different substrate concentrations spanning 2-200 μM. Substrate stock solutions were made up in dimethyl sulfoxide and added to the incubation such that the total concentration of DMSO was 0.5% (v/v) for all samples.

Incubations were performed at 37°C in a shaking water bath incubator. For assays involving HLC, 0.04 mg of total protein was used. For purified enzyme assays, 13 pmol of AO was used in each reaction. The reaction was initiated by addition of pre-warmed enzyme, run for a period of 5 minutes, and then quenched with 200 μl of 1 M formic acid containing a known concentration of the IS. Product formation was observed to be linear with respect to time for the reaction period of 5 minutes. The quenched samples were centrifuged for 10 min at 5000 rpm using an Eppendorf centrifuge 5415D, and the supernatant was collected for analysis.

Formation of the metabolite, DACA-9(10H)-acridone, was monitored by HPLC-MS/MS as previously described. [18] In brief, chromatographic separation was achieved using a Synergi Polar reverse-phase column (30 × 3.0 mm, 4 μm; Phenomenex, Torrance, CA) on an 1100 series HPLC (Agilent Technologies, Santa Clara, CA). The metabolite (DACA acridone) and the IS were detected on an API4000 triple quadrupole mass spectrometer (Applied Biosystems/MDS Sciex, Foster City, CA) using multiple reaction monitoring mode by monitoring the m/z transition from 310 to 265 and 161 to 120, respectively. Quantitation of product was accomplished by extrapolating from a standard curve ranging from 2 to 1000 nM of authentic DACA metabolite.

Enzyme kinetic parameters (V_{max}, K_m, and K_i) were determined by a non linear regression fit using the substrate inhibition equation shown below:

$$v = (V_{max}{}^{*}[S]) / (K_m + [S](1 + [S]/K_i))$$

where v is the reaction velocity, V_{max} is maximal reaction velocity, [S] is the substrate concentration, K_m is the Michaelis-Menten constant, and K_i is the inhibition constant for the substrate.

Statistical Analysis and Curve Fitting

Substrate saturation and peptide standard curves were plotted and analyzed using GraphPad Prism (version 4.03; GraphPad Software Inc., San Diego, CA). The substrate inhibition model was chosen as the best kinetic model according to the Akaike information criterion test that is built into Graphpad Prism. Other figures were generated using OriginPro (version 8.5.1; OriginLab Corp., Northampton, MA).

Results

Selection of Candidate Peptide

Digestion and subsequent MS analysis gave a sequence coverage of approximately 66% for human AOX1. From the numerous observed peptides, candidate peptides were selected based on three criteria. First, they must be unique for AOX1 when compared to the human protein database. Second, the peptides must be either singly or doubly charged. And last, the peptides must have a relatively high signal intensity. Ultimately, the peptide selected for this study was found to behave optimally in HLC with minimal signal interference and high sensitivity.

LC-MS/MS Quantitation Method

Figure 1 shows the structure of the peptide used for AO quantitation. A Q1 scan of the digested IS and native peptides showed an m/z of 500.1 and 497.1 respectively, corresponding to $(M+2H)^{2+}$. Product ion scans were taken for a digested sample containing both IS and native peptides. Spectra for product ion scan (MS2) are shown in Figure 2. Fragments were selected based on two criteria. First, the fragment monitored must contain the isotope labeled carbons, and secondly based on relative peak intensity. The first criterion was imposed as to limit the amount of interference between labeled and unlabeled peaks.

Three analogous MRM transitions were selected to monitor for both IS and native peptides. LC conditions were optimized to allow adequate separation of the peptide of interest away from contaminate peaks. Figure 3 shows a typical MRM chromatogram using digested purified AO containing IS. Despite the high selectively of MRM, contaminate peaks were observed due to the high complexity of the samples. In particular, one predominant contaminate peak was observed in the IS2 MRM channel. This was easily resolved however, due to the retention time of all peaks of interest being exactly the same (10.2 min).

Trypsin Digest of AO

A simple trypsin digest was developed and optimized for both digestion time and trypsin:protein ratios. The trypsin:protein ratio found to be optimal was 1:50 as an increase in relative trypsin did not increase peptide yields (data not shown). Figure 4A shows the effect of digestion time on peak area. With the exception of one MRM that was monitored, each peak had a maximum area after 11 hours of digestion; however, it was shown that the overall area ratio (and therefore measured concentration of peptide) remained consistent for

all digest times (Figure 4B). Although the largest signal was observed after 11 hours of digestion, many samples were run for closer to 16 hours for convenience. It has been reported that the addition of organic solvent to the trypsin digestion buffer may lead to greater yields for some peptides; [22, 23] however, addition of 10% acetonitrile into the digestion solution did not show any effect.

Purified Enzyme Curve

Purified AO was diluted, digested and analyzed for AO content. Figure 5B shows a typical UV spectra of purified AO. Determination of enzyme purity by sodium dodecylsulfate-polyagarose gel electrophoresis (SDS-PAGE) is challenging for AO due to the presence of degradation products of the enzyme that are formed under the reductive conditions of the method. However, a simpler method for estimating AO purity involves the comparison of the UV absorbance at 450 nm to the absorbance at 280 nm, effectively comparing the UV absorption of flavin to the absorption of bulk protein. Generally a value of 4-6 is indicative of a highly pure enzyme source. [15, 24] For both batches of recombinant enzyme, the 280:450 nm absorbance ratio was approximately 5, indicating a highly pure sample.

Figure 5A compares the concentration of AO measured by the MS assay versus calculated AO content by the UV_{450} assay. Linearity across a wide concentration range was observed ($r^2 = 0.99$). Figure 5C shows the comparison of the UV assay versus the MS assay for two different purified enzyme preparations. In general, the average MS measurement was approximately 40-60% of the corresponding UV measurement, depending on the batch. It should also be noted that UV quantitation is only viable in a highly purified system, as any UV spectra in a complex matrix would have too much interference.

Validation of Quantification

In order to demonstrate the validity of the assay in a complex sample matrix, a spiking experiment was performed. Figure 6 shows the comparison of HLC and purified measured individually (left) versus HLC and purified enzyme in the same sample (right). The graph illustrates that the recovered yield for the spiked sample was quantitative.

Undigested human liver cytosol and digested guinea pig liver cytosol were used as negative controls and no analyte peak was observed (data not shown). Guinea pig cytosol was selected as an appropriate negative control as it contains AOX1 but the peptide sequence differs in the region that was used for human AO quantification (EIDQTPYK for the human AOX1 sequence and GTEQTHYG for the corresponding region of the aligned guinea pig AOX1 sequence).

Determination of Method Detection Limit

The method detection limit (MDL) was calculated using a multiple injection method as described in detail in the methods section. The standard deviation in peak area of the chromatogram traces over five injections was used to calculate a MDL. Using the least sensitive MRM transition and thereby providing a conservative estimate, the MDL was determined to be 22 nM. However, when the most sensitive MRM transition is used for this analysis, the MDL is 6 nM.

Enzyme Kinetics

Steady state enzyme kinetics using purified AOX1 and 3 different pooled HLC batches were performed with DACA as the probe substrate. Table 1 shows the kinetic parameters for all enzyme sources. As one might predict, K_m was nearly identical between sources. However, a large difference in k_{cat}, and thus k_{cat}/K_m, values was observed, between purified (k_{cat}/K_m of 1.4) and HLC (k_{cat}/K_m of 15-20) indicating HLC to be 11-14 times more efficient in the

turnover of DACA than the E. coli expressed enzyme. Considerable batch to batch variation was also observed in HLC for V_{max} (3.3-4.9 nmol min^{-1} mg^{-1}) and k_{cat} (110-170 min^{-1}). Figure 7 shows the saturation kinetics for the four enzyme sources using substrate inhibition as the best fit model.

V_{max} values for DACA oxidation in HLC compared reasonably well with values in a previous study (average of 5.8 nmol $min^{-1}mg^{-1}$ over 4 donors), however the K_m observed appears to be lower (average of 28 μM over the same 4 donors). [25] Also, the previous report did not observe substrate inhibition.

Discussion

The exact physiological function of AO in humans is unknown. However, many recent findings suggest that AO has a broad biological importance. For example, it is known that AO can convert nitrite to nitric oxide during ischemia, producing physiological levels similar, or higher, than those seen for constitutive nitric oxide synthase. [26] AO has also been shown to play a role in toxicology in that metabolites produced by oxidation of azoheterocyclic structures leads to insoluble products similar to those seen for the uric acid product of the related xanthine oxidase enzyme. Other toxicological concerns revolve around the production of reactive oxygen species (ROS) by AO. Finally the role of AO in drug metabolism appears to be growing. [27] Thus, the levels of AO protein in human tissue are of importance for physiological, toxicological and pharmacokinetic reasons. Presently no literature method exists for determining the amount of AO protein in complex biological mixtures, and, as such, we have developed an effective methodology for AO quantitation in human subcellular fractions.

LC MS/MS methodology has been proven effective for quantitation of a variety of enzymes including cytochromes P450 and UDP-glucuronosyltransferases, [28] glutathione S-tranferases, [29] and carboxylesterases. [30] A recent review has described this stable isotope dilution (SID) approach as the gold standard in quantitation of proteins by MS. [31] Herein, we have applied this technique to develop a rapid, selective, and robust method achieving absolute AO quantitation. The method exhibits a linear signal response over a wide range of analyte concentration, as well as demonstrated to be highly specific for the peptides of interest in a complex sample matrix. Of the three batches tested, the lowest observed AOX1 concentration in HLC was 430 nM which was approximately 20 times the method detection limit (6-22 nM). Given the low MDL, researchers should be able to adapt this method in other tissues with lower levels of AO than human liver cytosol.

One important distinction in the approach within this paper compared to other literature methods is that the IS peptide is added to the solution and digested alongside the native proteins rather than being added post digestion. Figure 4a shows that digestion with trypsin releases free peptides in a time dependent way, and after a certain point, degradation of the sample begins. However, the curve also shows that trypsin digests both IS and native peptides without bias. In other words, trypsin cleaves (and other processes degrade) the smaller IS peptide at the same rate as the native peptide is cleaved from AO protein. As a result, the error in absolute quantitation due to incomplete digestion or over digestion is largely mitigated in this study.

As a way to verify our method, we quantified purified recombinant AO using both the MS assay and the UV_{450} detection assay. Figure 5a shows a linear relationship (r^2=0.99) between methods across a wide concentration range. However, it was found that the UV results were 1.7-2.5 fold higher than the results of the MS method. The exact reason for the discrepancy is unclear; however it may be due to the presence of background absorbance in

the UV assay causing a high reading. Given the relative imprecision of UV in general, an agreement within 2-fold provided us with confidence in our method.

Measuring the absolute AO concentration in HLC has allowed a k_{cat} value to be calculated for the first time using an unpurified native enzyme source. These k_{cat} values allow for a direct comparison between enzyme sources such as E. coli expressed enzymes or AO produced by cell culture with the native enzyme and native liver enzyme. This is important since AO has 4 different cofactors and depends on a number of enzymes to produce an active enzyme, [15] and it is expected that over expression might lead to lower levels of active enzyme relative to total protein. The k_{cat} values for DACA in purified AO are 13 min^{-1} while those for the native enzyme are a 170 min^{-1}. Thus while the K_m values are the same the relative k_{cat}/K_m values indicate that the efficiency of AO in HLC is approximately 15 times greater than purified. This is likely explained by incomplete MoCo incorporation, sulfurization, iron incorporation, and dimerization of the protein as it is expressed in E. coli cells. One enzyme in particular, MoCo sulfurase, plays a crucial role in modifying AO into its fully active form in humans. This enzyme incorporates a terminal sulfido ligand to the MoCo of both XO and AO, allowing for a functional enzyme. Clearly, some native sulfurase is present in the E. coli (TP 1000 cells) but the extent of sulfur incorporation is around a modest 30%. [15] Attempts by Hartmann and coworkers were made to increase overall enzyme activity by co-expressing human MoCo sulfurase along with AO but have proved unsuccessful. Although recent progress has been made, it seems there still exists an opportunity for further optimization of the heterologous expression of AO.

It is widely understood that some HLC preparations and hepatocytes show differing levels of enzyme activity. The origin of this difference is not understood and could be related to different preparation methods, enzyme denaturation, or desulfurization of the MoCo. Thus, a method to normalize protein levels will answer some of these questions and lead to more consistent comparisons of AO activities between different laboratories. Furthermore, it is not known if AO protein levels are under any translational regulatory control in humans, although adiponectin levels may play a role. [3] This methodology will allow for the determination of absolute AO levels across populations and may lead to an understanding of the importance of translational control on the protein levels of AO. As a proof of concept the difference in AO protein levels between various batches of human liver cytosol were determined. To that end, three different cytosol batches were analyzed for AO content (Table 1), and the variation between batches was found to be 21-40 pmol AOX1/mg total protein. Linear regression analysis for this small data set (n=3) showed a slight correlation between AOX1 levels and V_{max} ($r^2 = 0.48$). It is possible that a contributing factor to variation in HLC batches may be differences in preparation, storage, and handling. One study suggests that AOX1 activity may decline rapidly with storage or in post mortem tissues. [32] Also, the effects of buffer components, homogenization techniques, etc. in the preparation of liver cytosol may have some effect on activity. However, since the cytosol batches used in the current study came from the same vendor, most of these effects should be small. Further controlled studies may be beneficial to understand these effects, as the stability of the enzyme in cytosol under various conditions has not been explored.

Quantitation of AO protein should enable the advancement of AO research on multiple fronts. To date the tissue distribution of AO has not been determined at the protein level, and what is known depends solely on mRNA levels in different tissues. [14] Identifying the AO tissue distribution may provide insight leading towards the understanding of the physiological role of AO in humans. Additionally, quantifying protein levels in extrahepatic tissues may lead to better physiologically based pharmacokinetic (PBPK) models for AO, as it has been suggested that extrahepatic AO metabolism may explain extremely high clearance values (ie. exceeding hepatic blood flow) for some compounds found in the

literature. [16, 33, 34] Understanding the extrapolation of one in vitro AO source to another (eg. recombinant AOX1 to cytosol) may also aid in pharmacokinetic model development. Finally, this MS approach may also be extended to quantitation of AO in other species. The particular peptide used in this study shares 100% sequence identity with a number of different species including cow, horse, and various types of monkeys. This may contribute to the further understanding of interspecies differences in AO function and activity.

In conclusion, we have developed a highly selective, robust method for the quantification of AOX1 in HLC using a trypsin digest followed by LC-MS/MS analysis. The equipment needed is readily available in most labs and does require access to purified enzyme. Knowing the absolute AO concentration, we were able to measure k_{cat} in HLC, which is approximately 15 times greater than E. coli expressed purified enzyme. Different commercial HLC lots prepared from the same vendor show variations in AO content by as much as 2 fold, and a modest correlation between AO concentration and V_{max} was observed. This method may help explain donor to donor variation in AO activity, as well as provide a means to scale between different in vitro enzyme sources (eg. recombinant AOX1 to cytosol). In addition, this approach may be extended to other species and tissue types, leading to the development of physiologically based pharmacokinetic models and further investigation of the biochemical functions of this enzyme.

Acknowledgments

Funding. This work was supported by the National Institutes of Health National Institute of General Medical Sciences grant GM100874.

Abbreviations and Textual Footnotes

AO	aldehyde oxidase
AOX1	human aldehyde oxidase
MoCo	molybdenum cofactor
ROS	reactive oxygen species
DACA	N-[(2-dimethylamino)ethyl]acridine-4carboxamide
HPLC	high performance liquid chromatography
MS	mass spectrometry
ESI	electrospray ionization
IS	internal standard
MDL	method detection limit
PBPK	physiologically based pharmacokinetic
SDS-PAGE	sodium dodecylsulfate- polyagarose gel electrophoresis

References

1. Garattini E, Mendel R, Romao MJ, Wright R, Terao M. Mammalian molybdo-flavoenzymes, an expanding family of proteins: structure, genetics, regulation, function and pathophysiology. Biochem J. 2003; 372(Pt 1):15–32. [PubMed: 12578558]
2. Weigert J, Neumeier M, Bauer S, Mages W, Schnitzbauer AA, Obed A, Groschl B, Hartmann A, Schaffler A, Aslanidis C, Scholmerich J, Buechler C. Small-interference RNA-mediated knock-down of aldehyde oxidase 1 in 3T3-L1 cells impairs adipogenesis and adiponectin release. FEBS Lett. 2008; 582(19):2965–72. [PubMed: 18671973]

3. Neumeier M, Weigert J, Schaffler A, Weiss TS, Schmidl C, Buttner R, Bollheimer C, Aslanidis C, Scholmerich J, Buechler C. Aldehyde oxidase 1 is highly abundant in hepatic steatosis and is downregulated by adiponectin and fenofibric acid in hepatocytes in vitro. Biochem Biophys Res Commun. 2006; 350(3):731–5. [PubMed: 17022944]
4. Polyzos SA, Kountouras J, Zavos C. The multi-hit process and the antagonistic roles of tumor necrosis factor-alpha and adiponectin in non alcoholic fatty liver disease. Hippokratia. 2009; 13(2): 127. author reply 128. [PubMed: 19561788]
5. Ambroziak W, Izaguirre G, Pietruszko R. Metabolism of retinaldehyde and other aldehydes in soluble extracts of human liver and kidney. J Biol Chem. 1999; 274(47):33366–73. [PubMed: 10559215]
6. Schwartz R, Kjeldgaard NO. The enzymic oxidation of pyridoxal by liver aldehyde oxidase. Biochem J. 1951; 48(3):333–7. [PubMed: 14820867]
7. Kundu TK, Velayutham M, Zweier JL. Aldehyde oxidase functions as a superoxide generating NADH oxidase: an important redox regulated pathway of cellular oxygen radical formation. Biochemistry. 2012; 51(13):2930–9. [PubMed: 22404107]
8. Berger R, Mezey E, Clancy KP, Harta G, Wright RM, Repine JE, Brown RH, Brownstein M, Patterson D. Analysis of aldehyde oxidase and xanthine dehydrogenase/oxidase as possible candidate genes for autosomal recessive familial amyotrophic lateral sclerosis. Somat Cell Mol Genet. 1995; 21(2):121–31. [PubMed: 7570184]
9. Shaw S, Jayatilleke E. Ethanol-induced iron mobilization: role of acetaldehyde-aldehyde oxidase generated superoxide. Free Radic Biol Med. 1990; 9(1):11–7. [PubMed: 2170242]
10. Ali S, Pawa S, Naime M, Prasad R, Ahmad T, Farooqui H, Zafar H. Role of mammalian cytosolic molybdenum Fe-S flavin hydroxylases in hepatic injury. Life Sci. 2008; 82(13-14):780–8. [PubMed: 18313080]
11. Akabane T, Tanaka K, Irie M, Terashita S, Teramura T. Case report of extensive metabolism by aldehyde oxidase in humans: pharmacokinetics and metabolite profile of FK3453 in rats, dogs, and humans. Xenobiotica. 2011; 41(5):372–84. [PubMed: 21385103]
12. Diamond S, Boer J, Maduskuie TP Jr. Falahatpisheh N, Li Y, Yeleswaram S. Species-specific metabolism of SGX523 by aldehyde oxidase and the toxicological implications. Drug Metab Dispos. 2010; 38(8):1277–85. [PubMed: 20421447]
13. Zhang X, Liu HH, Weller P, Zheng M, Tao W, Wang J, Liao G, Monshouwer M, Peltz G. In silico and in vitro pharmacogenetics: aldehyde oxidase rapidly metabolizes a p38 kinase inhibitor. Pharmacogenomics J. 2011; 11(1):15–24. [PubMed: 20177421]
14. Garattini E, Terao M. Increasing recognition of the importance of aldehyde oxidase in drug development and discovery. Drug Metab Rev. 2011; 43(3):374–86. [PubMed: 21428696]
15. Hartmann T, Terao M, Garattini E, Teutloff C, Alfaro JF, Jones JP, Leimkuhler S. The impact of single nucleotide polymorphisms on human aldehyde oxidase. Drug Metab Dispos. 2012; 40(5): 856–64. [PubMed: 22279051]
16. Hutzler JM, Yang YS, Albaugh D, Fullenwider CL, Schmenk J, Fisher MB. Characterization of aldehyde oxidase enzyme activity in cryopreserved human hepatocytes. Drug Metab Dispos. 2012; 40(2):267–75. [PubMed: 22031625]
17. Alfaro JF, Joswig-Jones CA, Ouyang W, Nichols J, Crouch GJ, Jones JP. Purification and mechanism of human aldehyde oxidase expressed in Escherichia coli. Drug Metab Dispos. 2009; 37(12):2393–8. [PubMed: 19741035]
18. Barr JT, Jones JP. Evidence for substrate-dependent inhibition profiles for human liver aldehyde oxidase. Drug Metab Dispos. 2013; 41(1):24–9. [PubMed: 22996261]
19. Palmer T, Santini CL, Iobbi-Nivol C, Eaves DJ, Boxer DH, Giordano G. Involvement of the narJ and mob gene products in distinct steps in the biosynthesis of the molybdoenzyme nitrate reductase in Escherichia coli. Mol Microbiol. 1996; 20(4):875–84. [PubMed: 8793883]
20. Branzoli U, Massey V. Preparation of aldehyde oxidase in its native and deflavo forms. Comparison of spectroscopic and catalytic properties. J Biol Chem. 1974; 249(14):4339–45.
21. Wells, G.; Prest, H.; Russ, CW. Signal, Noise, and Detection Limits in Mass Spectrometry. Technical Note for Agilent Technologies Inc.; 2011. (Publication 5990-7651EN)

22. Miliotis T, Ali L, Palm JE, Lundqvist AJ, Ahnoff M, Andersson TB, Hilgendorf C. Development of a highly sensitive method using liquid chromatography-multiple reaction monitoring to quantify membrane P-glycoprotein in biological matrices and relationship to transport function. Drug Metab Dispos. 2011; 39(12):2440–9. [PubMed: 21949244]

23. Strader MB, Tabb DL, Hervey WJ, Pan C, Hurst GB. Efficient and specific trypsin digestion of microgram to nanogram quantities of proteins in organic-aqueous solvent systems. Anal Chem. 2006; 78(1):125–34. [PubMed: 16383319]

24. Stell JG, Warne AJ, Lee-Woolley C. Purification of rabbit liver aldehyde oxidase by affinity chromatography on benzamidine sepharose 6B. J Chromatogr. 1989; 475:363–72. [PubMed: 2777961]

25. Schofield PC, Robertson IG, Paxton JW. Inter-species variation in the metabolism and inhibition of N-[(2'-dimethylamino)ethyl]acridine-4-carboxamide (DACA) by aldehyde oxidase. Biochem Pharmacol. 2000; 59(2):161–5. [PubMed: 10810450]

26. Li H, Kundu TK, Zweier JL. Characterization of the magnitude and mechanism of aldehyde oxidase-mediated nitric oxide production from nitrite. J Biol Chem. 2009; 284(49):33850–8. [PubMed: 19801639]

27. Pryde DC, Dalvie D, Hu Q, Jones P, Obach RS, Tran TD. Aldehyde oxidase: an enzyme of emerging importance in drug discovery. J Med Chem. 2010; 53(24):8441–60. [PubMed: 20853847]

28. Ohtsuki S, Schaefer O, Kawakami H, Inoue T, Liehner S, Saito A, Ishiguro N, Kishimoto W, Ludwig-Schwellinger E, Ebner T, Terasaki T. Simultaneous absolute protein quantification of transporters, cytochromes P450, and UDP-glucuronosyltransferases as a novel approach for the characterization of individual human liver: comparison with mRNA levels and activities. Drug Metab Dispos. 2012; 40(1):83–92. [PubMed: 21994437]

29. Zhang F, Bartels MJ, Stott WT. Quantitation of human glutathione S-transferases in complex matrices by liquid chromatography/tandem mass spectrometry with signature peptides. Rapid Commun Mass Spectrom. 2004; 18(4):491–8. [PubMed: 14966858]

30. Sato Y, Miyashita A, Iwatsubo T, Usui T. Simultaneous absolute protein quantification of carboxylesterases 1 and 2 in human liver tissue fractions using liquid chromatography-tandem mass spectrometry. Drug Metab Dispos. 2012; 40(7):1389–96. [PubMed: 22504157]

31. Liebler DC, Zimmerman LJ. Targeted quantitation of proteins by mass spectrometry. Biochemistry. 2013; 52(22):3797–806. [PubMed: 23517332]

32. Duley JA, Harris O, Holmes RS. Analysis of human alcohol- and aldehyde-metabolizing isozymes by electrophoresis and isoelectric focusing. Alcohol Clin Exp Res. 1985; 9(3):263–71. [PubMed: 3893198]

33. Zientek M, Jiang Y, Youdim K, Obach RS. In vitro-in vivo correlation for intrinsic clearance for drugs metabolized by human aldehyde oxidase. Drug Metab Dispos. 2010; 38(8):1322–7. [PubMed: 20444863]

34. Jones JP, Korzekwa KR. Predicting intrinsic clearance for drugs and drug candidates metabolized by aldehyde oxidase. Mol Pharm. 2013; 10(4):1262–8. [PubMed: 23363487]

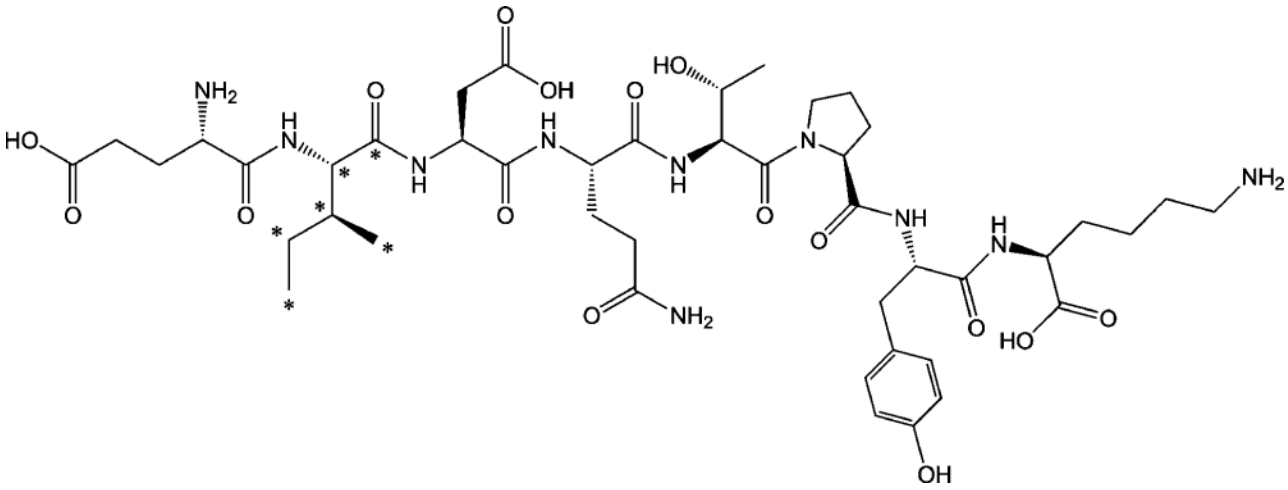

Figure 1.

Chemical structure of the digested peptide used for AOX1 quantitation. Asterisks indicate the ^{13}C labeled carbons in the internal standard peptide. IS and native peptides showed an m/z of 500.1 and 497.1 respectively, corresponding to $(M+2H)^{2+}$.

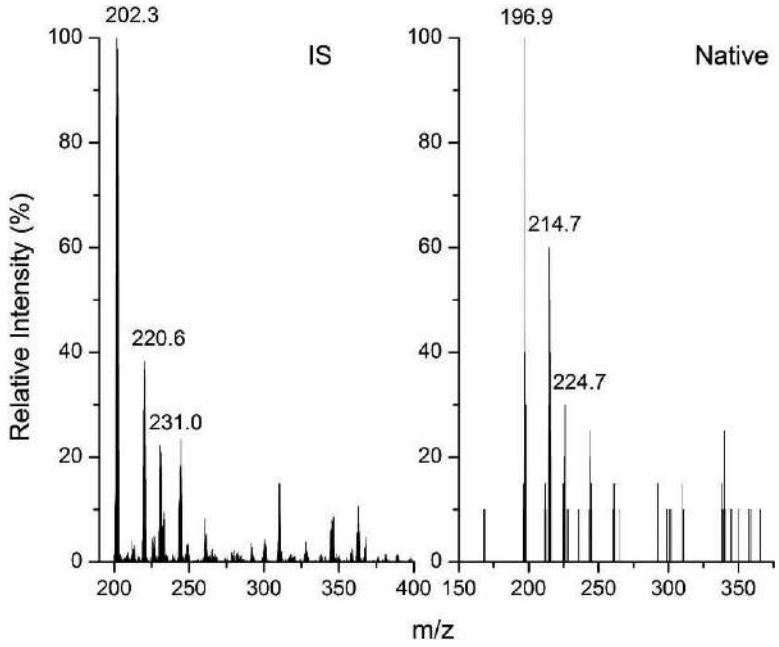

Figure 2.
Product ion (MS2) spectra displaying the fragmentation pattern for internal standard (left) and native (right) peptides.

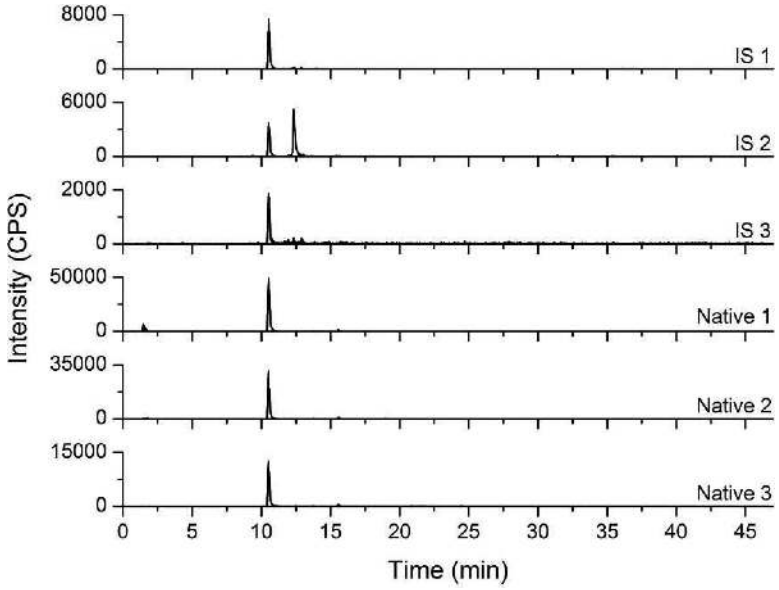

Figure 3.

HPLC/ESI-MS/MS chromatogram for purified AOX1 (native) and IS peptides after trypsin digestion. Three different fragmentation patterns for each peptide were monitored simultaneously using MRM mode: 500.1/202.3 (IS 1), 500.1/220.6 (IS 2), 500.1/231.0 (IS 3), 497.1/196.9 (Native 1), 497.1/214.7 (Native 2), 497.1/224.7 (Native 3).

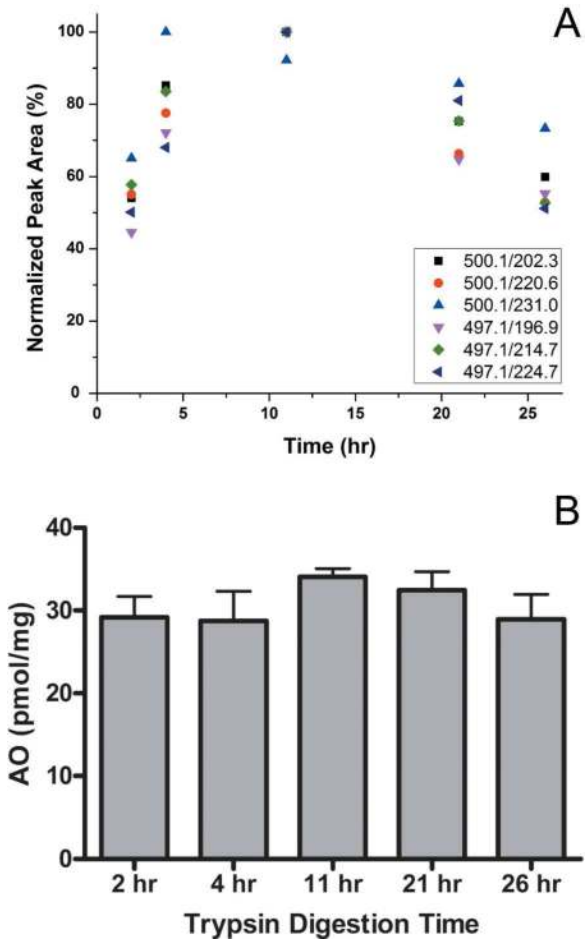

Figure 4.

A) Normalized peak area for each monitored MRM transition. Maximum peak areas were observed at 11 for 5 out of 6 MRM transitions. B) Effect of trypsin digestion time on absolute AOX1 concentration for a HLC sample. Bars represent the mean and error bars denote the S.E. for three different MRM transitions.

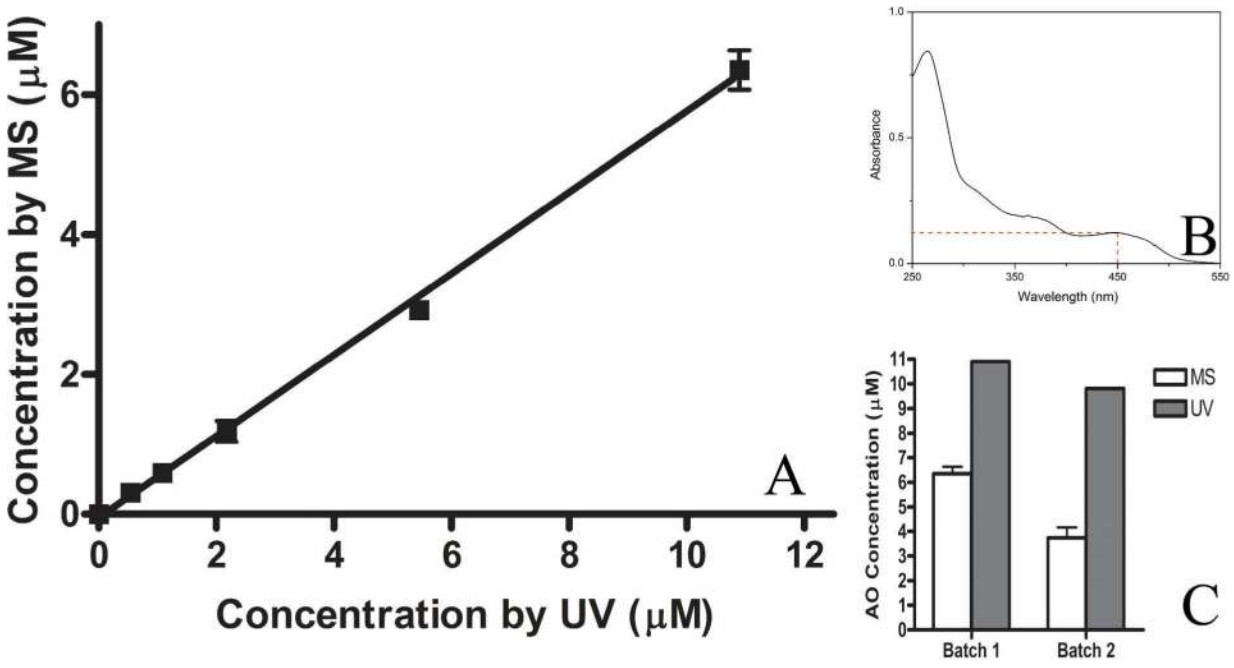

Figure 5.

A) Comparison of the measured AOX1 concentration values obtained using LC-MS method (y-axis) versus the direct UV method (x-axis) in purified enzyme source. B) A typical UV-Vis spectrum of purified aldehyde oxidase. AOX1 concentration was calculated via the absorbance measured at 450 nm using an extinction coefficient of 34.7 $cm^{-1}mM^{-1}$. C) Comparison of concentration between UV method and MS method for two batches of recombinantly expressed purified enzyme.

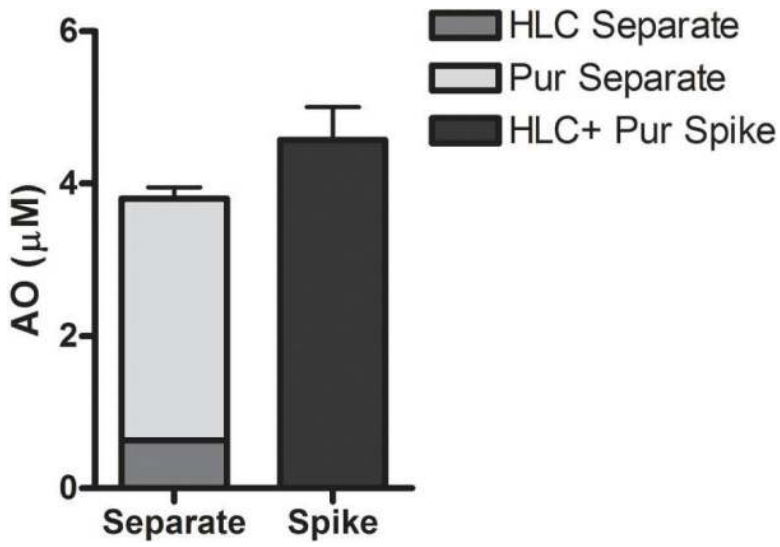

Figure 6.

Recovery of purified AOX1 from a spiked sample. Bar on left shows the measured AOX1 concentration for HLC and purified AOX1 samples measured separately while the bar on right shows the same HLC and purified samples measured in the same sample. Bars represent the mean and error bars denote the S.E. for three different MRM transitions.

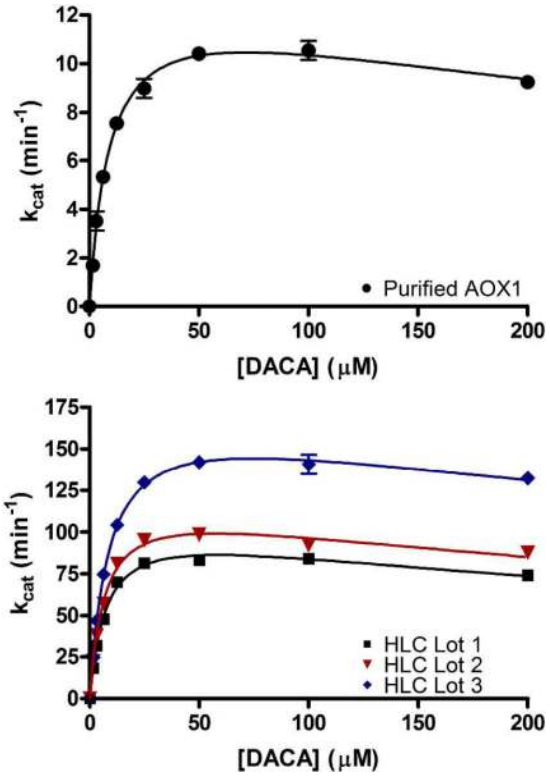

Figure 7.

Kinetic plots for multiple enzyme sources. Saturation plots for DACA oxidation in purified enzyme (top) and three batches of human liver cytosol (bottom) are shown. Such that all enzymes could be compared, k_{cat} vs substrate concentration is shown. Substrate inhibition was found to be the best fit model of the data. Points represent the mean, and error bars show the S.E. for duplicate measurements.

Table 1

AOX1 concentrations and saturation kinetic parameters for purified AOX1 and multiple lots of commercial HLC. AOX1 concentrations are the average of measurements ± S.D. made using three MRM transitions. Values for kinetics reflect the mean ± S.D. for duplicate experiments.

	[AO] *pmol/mg*	[AO] *μM*	V_{max} *nmol min^{-1} mg^{-1}*	K_i *μM*	K_{cat} *min^{-1}*	K_m *μM*	K_{cat}/K_m *min^{-1} μM^{-1}*
Purified	ND	6.4	ND	570 ± 140	13 ± 0.39	9.3 ± 1.1	1.4 ± 0.12
HLC Lot # 1	31	0.62	3.3 ± 0.16	480 ± 95	110 ± 5.1	7.3 ± 0.66	15 ± 0.64
HLC Lot # 2	40	0.79	4.9 ± 0.05	500 ± 30	120 ± 1.2	6.7 ± 0.14	19 ± 0.21
HLC Lot # 3	21	0.43	3.7 ± 0.02	640 ± 77	170 ± 1.1	8.7 ± 0.22	20 ± 0.38